Optical sampling to enhance Nyquist-shaped signal detection under limited receiver bandwidth

Geng, Zihan; Kong, Deming; Rozental, Valery; Lowery, Arthur James; Corcoran, Bill

Published in:
Optics Express

Link to article, DOI:
10.1364/OE.27.024007

Publication date:
2019

Document Version
Publisher's PDF, also known as Version of record

Research Article | Vol. 27, No. 17 | 19 Aug 2019 | OPTICS EXPRESS 24007
Optics EXPRESS

Optical sampling to enhance Nyquist-shaped signal detection under limited receiver bandwidth

ZIHAN GENG,[1,2] DEMING KONG,[1,2,3] VALERY ROZENTAL,[1,4] ARTHUR JAMES LOWERY,[1,2] AND BILL CORCORAN[1,2,*]

[1]*Electro-Photonics Laboratory, Department of Electrical and Computer Systems Engineering, Monash University, VIC 300, Australia*
[2]*Centre for Ultrahigh-bandwidth Devices for Optical Systems (CUDOS), Australia*
[3]*Now with: DTU Fotonik, Department of Photonics Engineering, Technical University of Denmark, 2800 Kgs., Denmark*
[4]*Now with: Toga Networks - Huawei, 4 HaHarash St. Neve Ne'eman, Hod Hasharon, Israel*
[*]*bill.corcoran@monash.edu*

Abstract: Insufficient receiver bandwidth destroys the orthogonality of Nyquist-shaped pulses, generating inter-symbol interference (ISI). We propose using an optical pre-sampler to alleviate the requirement on the receiver bandwidth through pulse re-shaping. Experiments and simulations using an optically shaped 40-Gbaud Nyquist-shaped on-off-keying signal (N-OOK) show receiver sensitivity improvements of 4- and 7.1-dB under 18- and 11-GHz receiver electrical bandwidths, respectively.

1. Introduction

Orthogonal multiplexing allows optical communication systems to efficiently occupy their available fiber bandwidth [1–3]. Nyquist-shaped signals, composed of overlapping pulses that satisfy Nyquist zero inter-symbol interference (ISI) criterion, such as sinc pulses, have a nearly rectangular spectrum, minimizing their spectral footprint [4–7]. Orthogonal pulse shaping has received significant attention in systems employing coherent detection (e.g. [2, 5]). Direct-detection systems have recently been of interest for short-reach optical communication systems, and orthogonal multiplexing can also be used in such systems (e.g. [3]). Ideally, these signals are received using direct detection without any ISI, if sampled at the ISI-free point, due to their time-domain orthogonality [3]. However, this orthogonality can be significantly degraded by electrical bandwidth limitations in the receiver.

Although it is well-known that when the receiver filter is matched to the transmitted signal, the receiver sensitivity is optimal [8–12], we are interested in the non-optimal case where the ratio (R) of the receiver's electrical bandwidth over the signal's baud rate is between 25% and 50%. This range is particularly interesting for study as a 50% bandwidth represents the minimum necessary bandwidth for coherent detection of optical Nyquist-shaped signals, and we expect ISI to play a major impact for any detection system below that bandwidth. In intensity modulated, direct detection (IM/DD) systems, bandwidth limitations have been extensively studied, and are again becoming relevant in a modern context for use in short-range and data-center links. Winzer and Kalmar [13] have developed a general theory for the receiver sensitivity under a number of bandwidths subject to return-to-zero (RZ) and non-return-to-zero (NRZ) coding. They show that, if the dominate noise source is signal-dependent, in the range of R between 25% and 50%, RZ coding provides at least a 3-dB benefit to receiver sensitivity compared with NRZ coding. This was of particular interest for optical time-division multiplexing (OTDM) systems, with optical demultiplexing via optical samplers intrinsically producing RZ pulses

#359151 https://doi.org/10.1364/OE.27.024007
Journal © 2019 Received 24 Apr 2019; revised 19 Jun 2019; accepted 24 Jun 2019; published 7 Aug 2019

Optics EXPRESS

before the receiver. Additionally, OTDM demultiplexing showed further sensitivity improvement by gating amplified spontaneous emission (ASE) noise [14]. Further practical considerations in OTDM demultiplexing, such as the gating window width and extinction ratio [15], have also been analyzed. These studies show that receiving signals on short optical pulses, either through optical sampling or RZ encoding, reduces signal degradation from ISI and ASE-ASE beating. However, while carrying data on short optical pulses is advantageous for receivers, such signals have a wide bandwidth, which can limit achievable signal throughput in wavelength division multiplexing. This then suggests that a system which transports Nyquist-shaped signals, but receives RZ coded signals, may simultaneously provide efficient spectral utilization, and reduced impairments from ISI.

In this work, we focus on bandwidth limited reception of Nyquist-shaped IM/DD signals. Nyquist-shaped signals are transmitted with high spectral efficiency, and at the receiver, they are converted to RZ-shaped signal for better sensitivity. A single photo-detector and optical sampling at one sample-per-symbol with a 33% duty-cycle sampling pulse are used in this work. Our assumption is the signal's baud rate is 2 to 4 times of the receiver's electrical bandwidth, in other words, the receiver's electrical bandwidth is 25% to 50% of the signal's baud rate. This is an extension paper of the work we presented at the Optical Fiber Communication Conference (OFC) [16], in which we discussed optical sampling of an electrically-shaped Nyquist on-off-keying (N-OOK) signal. In this paper, we focus on optical sampling of an optically shaped N-OOK signal and make further analysis into factors such as the optical sampling pulse width and the sharpness of the magnitude response of the receiver. Simulations show that optical pre-sampling can improve receiver sensitivity for optically-shaped N-OOK signals under a number of receiver bandwidths. In our proof-of-concept experiment, we use a 4×10-Gbaud orthogonal time division multiplexing (OrthTDM) signal to emulate an optically-shaped 40-Gbaud N-OOK signal and show that optical sampling can improve the sensitivity of a band-limited 18-GHz receiver by 4 dB.

2. Principle of operation

Figure 1 (a) shows three detection systems for optically shaped N-OOK with their eye diagrams and electrical spectra. With sufficient receiver bandwidth (upper system), there is a clear and short optimal sampling window for each symbol period, as observed in the eye diagram. If the receiver is bandwidth-limited (middle system), such that the receiver's electrical bandwidth is 25% to 50% of the signal's baud rate, there is significant degradation due to the attenuation of the high frequency components, causing ISI. In our proposed system (bottom system), the

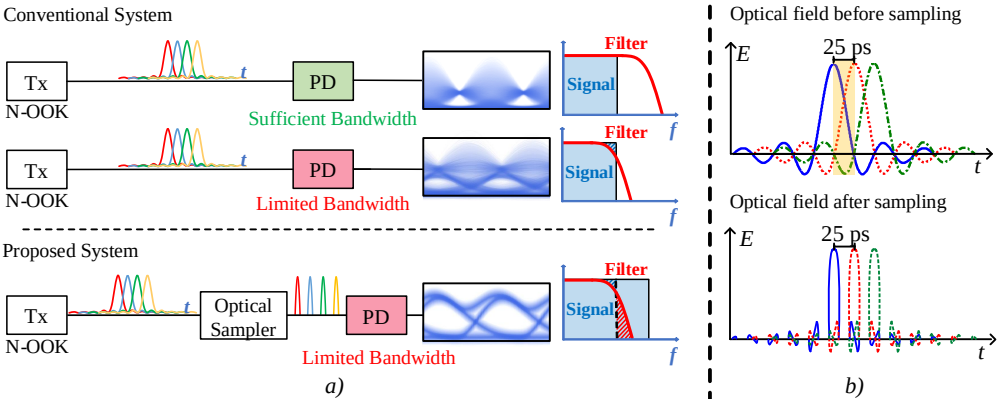

Fig. 1. (a) Principle of optical pre-sampling before bandwidth-limited receivers. (b) Optical field of optically shaped 40-Gbaud N-OOK before and after optical sampling.

Optics EXPRESS

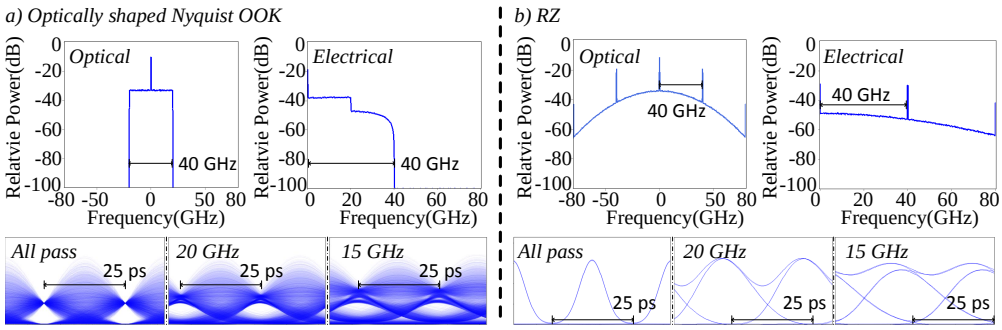

Fig. 2. Optical and electrical spectra and eye-diagrams of 40-Gbaud (a) optically shaped N-OOK and (b) RZ direct detection with no electrical band limitation, or with 20-GHz or 15-GHz 4th-order Bessel electrical low pass filter. The results are from a VPItransmissionMaker simulation without additional noise.

degradation due to insufficient bandwidth is reduced by the optical pre-sampler.

The optical sampling at one sample-per-symbol can be viewed in the frequency domain as a convolution of the signal spectrum and a frequency comb, leading to repeated frequency components and spectral "whitening" [17]. As indicated in the bottom row of Fig. 1(a), the repeated frequency components from the sampling operation allow for reshaping through filtering. In our previous works [18, 19], the repeated frequency components have been shown to increase tolerance to band-limiting effects of optical filters in transmission links. The effects observed in these previous investigations are conceptually similar to the effect of optical sampling and receiver electrical bandwidth limiting filters in this investigation.

Alternatively, this approach can be explained in the time domain. Figure 1(b) shows the envelope of the optical field of an optically shaped 40-Gbaud N-OOK signal [3, 20] before and after optical sampling. The envelope has negative excursions, which are π phase shifts to the optical carrier. As each '1' data bit is a sinc pulse with long tails that change sign from bit-slot to bit-slot, the tails of adjacent 1-bits will partially destructively interfere (e.g the blue and red traces), whereas 1-bits separated by two bit slots have tails that constructively interfere (e.g. the blue and green traces in Fig. 1(b)). Because the sincs have long tails, many 1-bits will contribute to the total field at a given instant; but zero bits will not contribute as they are encoded as zero power. Thus the total field will depend on the pattern of data sent. Fortunately, if there is no bandwidth limitation, the zero-crossing points of all of the tails align with the peak of the wanted pulse; this is the sampling time that will give zero-ISI. However, if the receiver has insufficient bandwidth, the low-pass filter (LPF) distorts the symbols, causing a loss of orthogonality between adjacent symbols, and there will not be a sampling time that will give zero-ISI. Optical sampling (that is, sampling before the photodiode (PD)-induced bandwidth limitation) selects the peak of the desired data-bit's sinc, and suppresses the tails of the preceding and following sincs away from the crossing points. Thus, there is very little energy left in the tails of the preceding and following sincs, energy that would have caused ISI after band-limiting. This means that the electrical waveform becomes much less dependent on the data pattern, reducing the variances of the traces corresponding to the 1 and 0 bits.

In this work, we used Gaussian pulses to sample optically shaped N-OOK signals. When the optical sampling pulses are significantly narrower than the bit-period of the N-OOK signal, the optically shaped N-OOK symbols are transformed into return-to-zero (RZ) symbols through optical sampling. If the sampling pulse width is equal to or less than 0.44× the symbol duration, the sampled signal is roughly RZ-shaped with some inter-symbol-interference from other symbols. In Fig. 2, optical spectra, electrical spectra and eye-diagrams of optically shaped 40-Gbaud N-OOK and 40-Gbaud RZ signals are compared. The bandwidth-limiting is modelled by a 4th-order Bessel electrical low-pass filters. In particular, the spectra shown in Fig. 2 can qualitatively

Optics EXPRESS

provide an explanation of ISI in direct-detection systems with limited receiver bandwidth. While in a coherent detection system, the electrical spectrum of the received signal is directly mapped from the optical signal, the spectra in Fig. 2(a) show that the optically shaped 40-Gbaud double side-band (DSB) N-OOK signal has a 40-GHz optical bandwidth centred around a carrier. If the electrical signal was solely due to the mixing of the carrier and the sidebands (as in coherent detection systems), a 20-GHz-wide electrical spectrum would be expected. However, additional frequency components are generated due to square-law photo-detection, causing mixing of all of the tones within both sidebands, to give a 40-GHz-wide electrical spectrum. As shown in the eye diagrams of Fig. 2(a), limiting the electrical bandwidth causes substantial ISI.

There are trade-offs in using N-OOK in DD systems. N-OOK signals have a well-confined optical spectrum, which is suitable for multiplexing, all-optical routing and elastic networks [6, 7]. However, as shown in Fig. 2(a), optically shaped N-OOK can be very sensitive to receiver bandwidth limitations, with the required electrical bandwidth exceeding the symbol rate for penalty-free reception. On the other hand, an RZ signal is less sensitive to limited receiver bandwidths, but an RZ signal occupies a much wider optical bandwidth during transmission, so limits the total achievable data rate by limiting the number of channels able to be multiplexed onto a given optical bandwidth. In this way, Nyquist-shaped signals are preferred for transmission, and RZ signals are more desirable for detection. Optical pre-sampling before photodetection combines the merits of both of them.

3. Simulation setup

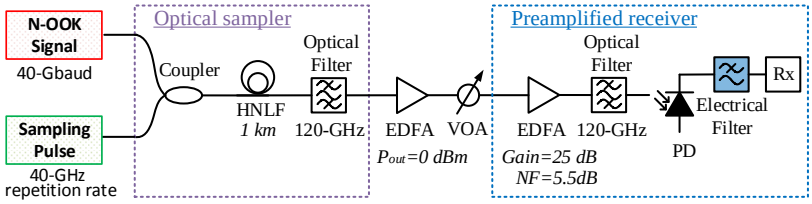

Fig. 3. Simulation Setup of receiver enhanced by optical pre-sampler. EDFA: erbium-doped fiber amplifier. VOA: variable optical attenuator. HNLF: highly nonlinear fiber.

Figure 3 shows the simulation setup for the optical pre-sampler. A 15^{th}-order pseudorandom binary sequence (PRBS) of 2^{18} bits is simulated for each BER calculation. The optically shaped N-OOK signal is generated by modulating a Gaussian-shaped ultra-short optical pulse train, whose repetition rate is 40-GHz, with a 40-Gbaud electrical non-return-to-zero (NRZ) signal, followed by a 40-GHz rectangular optical band-pass filter (BPF) [20]. A zero roll-off, optically shaped 40-Gbaud N-OOK signal ("signal") centered at 1550.9 nm, is optically sampled by 3.67-ps width (120-GHz bandwidth), 40-GHz repetition rate short Gaussian pulses ("pump") centered at 1547 nm, in a HNLF to generate the optically sampled signal ("idler") at a new frequency through the FWM process.

We simulate the sampling process using a HNLF to gain insight into the experiments presented in Sections 5 & 6. The HNLF is 1-km in length with a 1547-nm zero dispersion wavelength and 9.3 $W^{-1}\cdot km^{-1}$ non-linear coefficient. The conversion efficiency of the FWM is about -10 dB. The idler is extracted by a 120-GHz optical band pass filter, an idler power set to 0 dBm average power by a noiseless EFDA to simplify simulation.

The signal is then sent to an amplified receiver, where an attenuator varies the received optical power, and noise is added through amplification with an EDFA which has 25 dB gain and a 5.5 dB noise figure. This "back-to-back" set-up provides a general benchmark of receiver sensitivity, independent of the link placed before the receiver. We are assuming that our proposed system is primarily of interest for short-reach systems where OSNR is high. We further assume that in order to employ high bandwidth signals in a direct-detection system, optical dispersion compensation

Optics EXPRESS

is to be used. Under these assumptions, our results should provide a good indication of the sensitivity improvements enabled by our proposed optical sampling front-end.
The 3-dB bandwidth of the electrical low-pass filter (LPF) after the photodiode was switched between 11 to 62 GHz to emulate receiver bandwidth limitations, as shown in Fig. 4. The performance of systems with a sharp brick-wall rectangular filter (implemented as a 30th-order Gaussian filter, red traces in Fig. 4) and a slow roll-off filter (4th-order Bessel filter, blue traces in Fig. 4) are compared. The brick-wall filter resembles a digitally-defined filter used in some real-time digital oscilloscopes, and more generally the effect of anti-aliasing filters in receiver sampling front-ends. The Bessel filter is more typical of analog bandwidth limits (e.g. photodiode response). Note that the time-bandwidth product of the sampling pulses is 0.44, which is the transform limit for Gaussian pulses.

4. Simulation results

Figure 4 shows the simulated BER versus received optical power for signals and idlers under various electrical filter bandwidths. The Bessel filter (blue traces) and the rectangular filter (red traces) mentioned above are simulated. The solid lines represent signals without optical pre-sampling, and the dashed lines indicate idlers or optically sampled signals. We define the receiver sensitivity here as the required received power (average power into the preamplified reciever shown in Fig. 3) in order to reach a BER of 3.8×10^{-3}, assuming a commonly used second-generation, 7% overhead, concatenated hard-decision forward error correction (HD-FEC) code. When the receiver bandwidth is set by a 11-GHz Bessel filter, error-free operation below the FEC threshold can be achieved with optical sampling, providing 7.1-dB sensitivity improvement. When brick-wall filtering is applied, optical sampling provides no improvement and error-rates are well above the FEC threshold. Figures 4(b)-(e) show the performance with filter bandwidths between 18-22 GHz. For the brick-wall filter, optical sampling improves sensitivity by 9, 5.5, 4.1 and 2.2 dB for 18, 19, 20 and 22 GHz bandwidth filters, respectively. For the Bessel filter, the improvements are 3.8, 3.3, 3.1 and 2.8 dB for the same filter bandwidths, respectively. In Fig. 4, the traces for 62-GHz filters follow the same tendency, but there is a 3.3-dB sensitivity improvement from optical sampling. We attribute this base line sensitivity improvement to the RZ shaping [10–15]. Given the same average power, compared with the N-OOK signal, the low duty-cycle RZ signal has 3.3 times higher power for its "1" level.

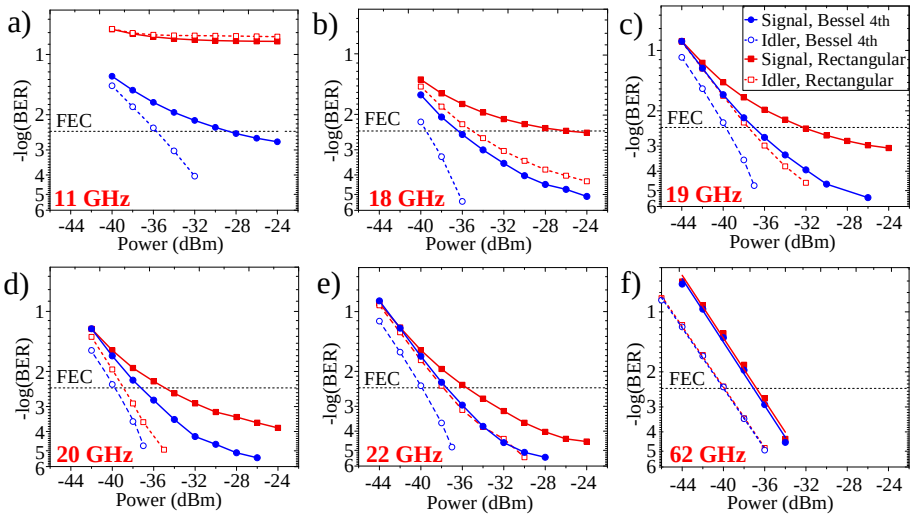

Fig. 4. Simulated BER versus received optical power plots for signals and idlers filtered by 4th order Bessel electrical filter (circles), and rectangular electrical filter (squares) after photo-detection. Filter bandwidths change with each sub-figure, as indicated on each.

Optics EXPRESS

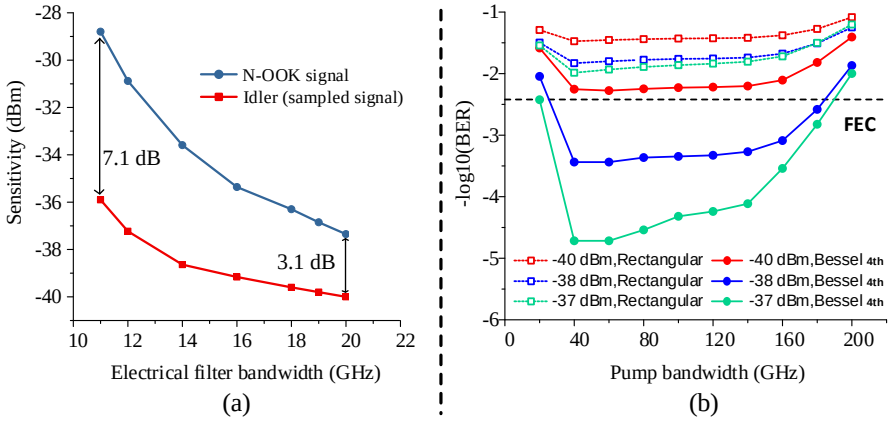

Fig. 5. (a) Sensitivity (received optical average power at BER = 3.8×10^{-3}) versus electrical filter bandwidth, with 120-GHz pump and 4th order Bessel electrical filter. (b) BER versus pump (sampling pulse) bandwidth, with 18-GHz low-pass 4th order Bessel electrical filter.

Figure 5(a) summarizes the sensitivity versus electrical filter bandwidth, when the receiver bandwidth is modelled as a 4$^{\mathbf{th}}$-order Bessel filter. The sampling pulse width is set to 3.67 ps, which corresponds to a 120-GHz pump bandwidth, and the electrical filter at the receiver is 4th-order Bessel filter. Comparing the two lines in Fig. 5(a), the optically shaped N-OOK signal requires a higher power for all bandwidths investigated. As the bandwidth is increased, the difference between the sensitivities for the sampled idler and the optically shaped N-OOK signal are reduced. This shows that, predictably, the optically shaped N-OOK signal has a larger penalty than the sampled signal (idler) as receiver bandwidth is reduced. The optical pre-sampler improves the receiver sensitivity by 3.1 dB for a 20-GHz electrical filter bandwidth, and 7.1 dB at 11-GHz bandwidth.

Figure 5(b) plots BER versus pump bandwidth. The measurement is taken with an 18-GHz low-pass 4th-order Bessel filter at the receiver. According to Fig. 5(b) optical sampling with 80-GHz pump bandwidth outperforms sampling with 120-GHz pump bandwidth, and this conclusion is consistent with our experimental results in the following section. When the pump bandwidth is less than 40 GHz, the sampling pulses with a repetition rate of 40 GHz start to overlap. Thus the optical sampling gate will not be completely closed. When the pump bandwidth is larger than 120-GHz, due to the optical and electrical filters in the system, the received signal power before the PD is reduced. In addition, as the increase of pump bandwidth, the spectra of the pump and idler may be partially overlapped. Among the parameters swept in the simulation, 40-GHz and 60-GHz bandwidths give maximum performance.

5. Experimental setup

We now validate the conclusions drawn from our simulations through a proof-of-concept experiment. Figure 6 shows the experimental setup of an optically shaped 40-Gbaud N-OOK transmitter and a receiver with an optical pre-sampler, which is conceptually similar to the simulation described in Section 3. The optically shaped 40-Gbaud N-OOK signal was sampled by short optical pulses with a 40-GHz repetition rate. The signal is emulated by time-division multiplexing of four optically shaped, 25% duty cycle, 10-Gbaud N-OOK signals. An ERGO mode-locked laser, centered at 1555.5 nm, generates frequency comb lines with 10-GHz spacing and 1.4-ps optical pulses. The frequency comb is amplified by an erbium-doped fiber amplifier (EDFA) to 21.8 dBm and spectrally broadened through self-phase modulation (SPM) in a normally-dispersive highly nonlinear fiber (HNLF) (508 m length, -0.5 ps/nm/km dispersion @ 1550 nm, 0.016 ps/nm^2/km dispersion slope @ 1550 nm, 11 W^{-1}·km^{-1} non-linear coefficient).

Optics EXPRESS

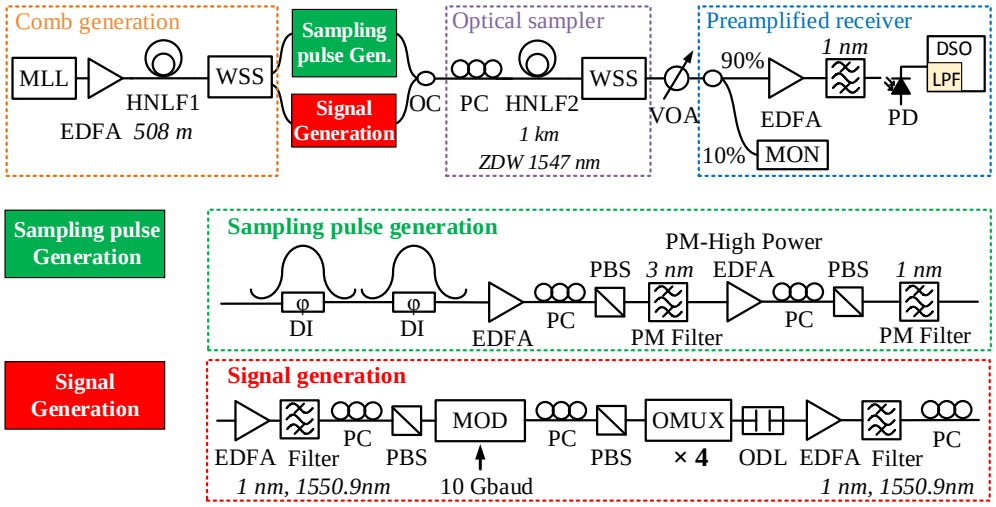

Fig. 6. Experimental setup of receiver enhanced by optical pre-sampling. MLL: mode-locked laser. MOD: modulator. WSS: wavelength selective switch. PC: polarization controller. PBS: polarization beam splitter. DI: delay line interferometer. OMUX: optical multiplexer. ODL: optical delay line. OC: optical coupler. MON: monitor. ZDW: zero dispersion wavelength. WDM: wave division multiplexing. PD: photodiode. DSO: digital sampling oscilloscope.

Two outputs of a wavelength selective switch (WSS) are used for the signal or sampling pulse generation.

The sampling pulse train is generated by filtering the 10-GHz spacing comb lines with the WSS and two delay-line interferometers, and it is centered at 1547 nm with a 40-GHz repetition rate.

Nyquist signals can be generated optically by either filtering modulated signals [6, 7, 20–23] or by modulating sinc-shaped optical pulses [3, 24–26]. These reduce the requirements on DSP and DACs, while being able to operate over very high bandwidths [22]. In this experiment, the optically shaped 40-Gbaud N-OOK signal is generated by modulation of the frequency comb and time division multiplexing. The WSS-filtered frequency comb with 40-GHz bandwidth, 10-GHz frequency comb spacing and 1550.9-nm center frequency, is intensity modulated by a 10-Gbaud PRBS-15 signal, and then de-correlated and time division multiplexed by 4 times with a Pritel optical clock multiplier. The intensity modulator is biased at quadrature point and driven to maximize the extinction ratio. The time alignment between the signal and gating pulses is achieved by tuning the variable optical delay line. Note that since the Nyquist-shaping WSS has a 10-GHz granularity, there is a deviation in the Nyquist-shaping filter responses between the experiment and the simulation. The influence on the experimental results will be discussed in Section 7.

The optical sampler is a 1-km HNLF with 1547 nm zero dispersion wavelength (ZDW), and 0.074 ps/nm^2/km dispersion slope at 1550 nm. The signal and pump powers at the input of the WDM coupler are 2.2 dBm and 15.5 dBm respectively. Polarization controllers are used to align the signal and pump polarizations for maximum FWM efficiency. A WSS extracts the idler by applying a Gaussian-shaped band-pass filter at 1543.1 nm with 120-GHz bandwidth.

In the pre-amplified receiver, a variable optical attenuator (VOA) sets the average power at the input of the pre-amplified receiver, and 10% of the power is monitored by a power meter. Before photodetection, a 1-nm optical BPF reduces out-of-band noise produced by the receiver EDFA pre-amplifier. The photodiode is a Finisar XPDV3120 70-GHz photodetector. In the digital

Optics EXPRESS

sampling oscilloscope (DSO), the sampling rate is 160 GSa/s. The anti-alias filter, which is a 9-bit FIR digital low-pass filter built into the oscilloscope, is switched between 18 and 62 GHz (Fig. 8).

6. Experimental results

Figure 7(a) shows the FWM spectra at the output of HNLF2 in blue. In the spectral domain, the idler carries the information of the signal with about -8 dB FWM conversion efficiency. The green and the red traces are the pump and signal before HNLF2. Comparing the three traces indicates the spectrum of the pump is broadened, and the signal's spectrum is shaped. We attribute pump broadening to SPM in the HNLF, and signal shaping due to a combination of SPM and cross-phase modulation (XPM) from the pump. We expect these processes to introduce some distortion on the idler. Figure 7(b) shows the electrical spectrum of the received idler limited by the 62-GHz LPF in the oscilloscope. This digital LPF has a sharp edge and a high extinction of 57 dB. The electrical spectrum fits well to a 0.02 roll-off raised-cosine filter response represented by a red dashed line. From the prior simulations, this brick-wall-like filter will have a strong effect on the received signal quality, dominating over the 70-GHz 3-dB bandwidth limit of the photodiode. Figure 7(c) shows the eye-diagram of an optically shaped N-OOK signal at -31 dBm average power detected by a 62-GHz electrical bandwidth receiver, which has sufficient bandwidth to detect the optically shaped 40-Gbaud N-OOK signal.

Figure 8 shows BER versus received optical power, as well as eye diagrams for the received optically sampled idler at -36 dBm average power. We plotted two separate curves for the idler, corresponding to Gaussian-shaped pumps with either 80- or 120-GHz bandwidths, which should

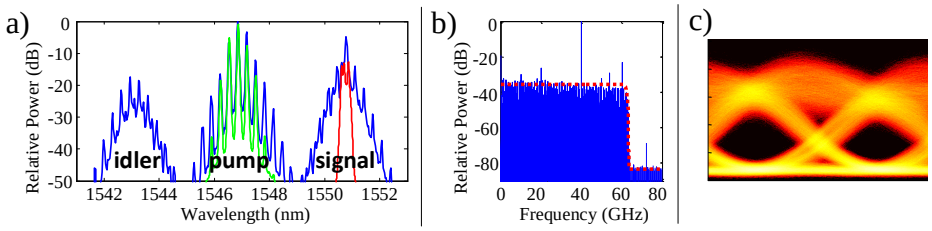

Fig. 7. (a) Red: spectrum of the signal before FWM process. Green: spectrum of the sampling frequency comb (pump) before FWM process. Blue: spectrum at the output of the HNLF2. (b) Electrical spectrum of the idler limited by 62-GHz electrical bandwidth.(c) Eye diagram of the 40-Gbaud N-OOK signal detected with 62-GHz electrical bandwidth receiver.

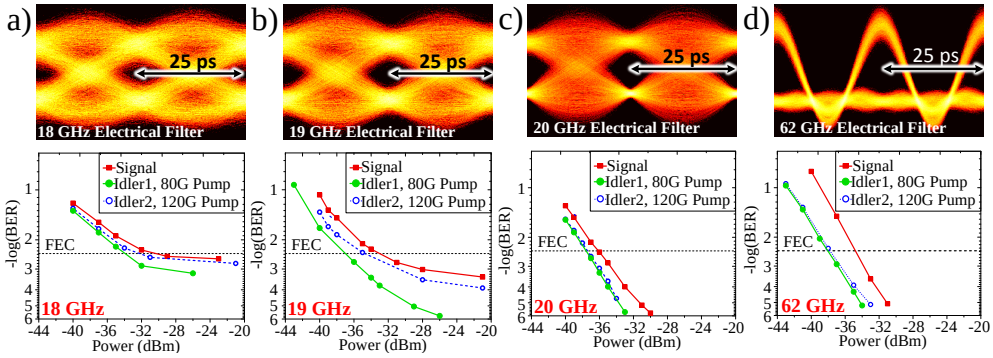

Fig. 8. Experimental eye-diagrams of signal optically sampled by a 80-GHz sampling pulse train (pump) at -36 dBm average power and BER versus received optical power curves for (a) 18-GHz (b) 19-GHz (c) 20-GHz (d) 62-GHz bandwidth-limited signal and idler.

Optics EXPRESS

ideally result in sampling pulses with 5.5-ps or 3.6-ps durations, respectively. We tested the performance with 18, 19, 20 and 62-GHz filters applied in the oscilloscope. For the 18-GHz and 19-GHz filters, the 120-GHz bandwidth sampling pulse produces worse sensitivity than the 80-GHz wide pulse (Figs. 8(a) and (b)), owing to the greater signal loss caused by the electrical and optical filters in the receiver.

For the 18- and 19-GHz bandwidth receiver filters, we measured a sensitivity improvement of 4 dB for pre-sampling. With the 20-GHz filter, this improvement drops to 2 dB. With a 62-GHz filter applied, the improvement from optical sampling increases to 3.8 dB. This we attribute to full conversion of the idler to an RZ signal (as illustrated by the eye diagram), alongside a large susceptibility of the signal to timing jitter in the receiver due to the signal's pulse shape.

7. Discussion

Both the simulation and the experiment show that, for receiver bandwidths less than half the signal symbol rate, optical pre-sampling can improve sensitivity in optically shaped N-OOK systems. The main contributor to the improvement is the N-OOK to RZ conversion, as indicated in the simulation, and a minor contributor could be the reduced noise-noise beating due to the noise being time-gated by optical sampling [27]. Comparing the simulation and the experiment, we note that there are other factors besides the receiver bandwidth and the sampling pulses that define the receiver sensitivity. Most factors affect the results of signal and idler similarly, except for the optical Nyquist-shaping filter response. In the experiment, the WSS for optical Nyquist-shaping is set to 40-GHz rectangular BPF, but it has a basic optical transfer function of a 10 GHz Gaussian. The resultant optical spectrum has a roll-off softer than the simulated ideal rectangular spectra. According to [3], the quasi-orthogonal property can be maintained in Nyquist pulses even when the roll-off is not zero, and the softer roll-off results in better tolerance to the bandwidth limitation. Therefore, compared with simulation, the optically shaped N-OOK signal in the experiment has better sensitivities, leading to reduced sensitivity improvements in the experiment. Note that we do not use any equalization stages in either simulations or experiments, with our receiver acting only as a simple threshold comparator. It may be possible to improve system performance through the use of an equalizer, at the cost of some computational complexity and processing latency. Moreover, the combination of optical sampling and equalization may enable Nyquist signal reception where equalization alone may not be sufficient for signal recovery.

There are several further challenges to be met in order to make our system of immediate use in installed communication systems. To use this proposed receiver in a densely packed Nyquist wavelength-division-multiplexed (NWDM) system, it requires sharp optical filtering such as a ring-assisted Mach-Zender interferometer (RAMZI), which we have previously demonstrated [22, 28]. For future mass production, the mode-locked laser and the HNLF in this work should be replaced with on-chip frequency combs [29] and on-chip optical sampling [30, 31]. Moreover, the sampler used for this function must be synchronized to the clock of the incoming signal. This can be achieved in synchronous systems, or through a clock recovery/synchronization stage [32], at the expense of some electronic control. These improvements also relate to reducing receiver complexity through integration onto a chip-based platform, which may help to reduce the extra costs expected in systems with increased complexity. Fundamentally, our proposal targets systems where the use of a higher bandwidth photodiode and electronic front end is either impractical or not possible, and a cost-benefit analysis should be done on that basis.

For further studies, it would be interesting to investigate the effect of optical sampling at one sample-per-symbol for coherent detection of Nyquist shaped signals, considering that parallel optical sampling has been shown to be advantageous for coherent detection [33, 34]. Moreover, the number of sampling stages in a WDM system might be reduced in a WDM receiver measuring multiple channels simultaneously. Ensuring that the sampled channels are sufficiently optically demultiplexed that upon sampling they do not spectrally overlap (causing inter-channel

Optics EXPRESS

interference) would be key, as would be the time domain synchronization of such channels. This is less likely to be of benefit in a system employing wavelength routing, where a per-channel front end is likely to be necessary.

8. Conclusion

We have experimentally demonstrated that the quality of a direct-detected, optically shaped 40-Gbaud Nyquist OOK signal can be improved by optical pre-sampling in a band-limited system, where the receiver bandwidths are below the single-sided bandwidth of the optical signal. Proof-of-concept experiments using FWM in an HNLF show a receiver sensitivity improvement of 4 dB with an 18-GHz electrical bandwidth receiver, where this bandwidth limiting is performed by a brick-wall anti-aliasing filter. Simulations show that with a 4^{th}-order Bessel filter, emulating analog component responses, it is possible for optical pre-sampling to improve receiver sensitivity of an 11-GHz bandwidth receiver by 7.1 dB. This work shows that when the receiver's electrical bandwidth is about 25% to 50% of the signal's baud rate, the sensitivity measured at the receiver can be improved by optical sampling, especially for Nyquist-shaped signals.

Funding

Australian Research Council (ARC) (CE110001018, FL130100041).

Acknowledgments

We acknowledge support from VPIphotonics under their universities program.

References

1. A. J. Lowery, L. B. Du, and J. Armstrong, "Performance of optical OFDM in ultralong-haul WDM lightwave systems," J. Light. Technol. **25**, 131–138 (2007).
2. G. Bosco, V. Curri, A. Carena, P. Poggiolini, and F. Forghieri, "On the performance of Nyquist-WDM terabit superchannels based on PM-BPSK, PM-QPSK, PM-8QAM or PM-16QAM subcarriers," J. Light. Technol. **29**, 53–61 (2011).
3. M. Nakazawa, T. Hirooka, P. Ruan, and P. Guan, "Ultrahigh-speed "orthogonal" TDM transmission with an optical Nyquist pulse train," Opt. Express **20**, 1129–1140 (2012).
4. G. Bosco, A. Carena, V. Curri, P. Poggiolini, and F. Forghieri, "Performance limits of Nyquist-WDM and CO-OFDM in high-speed PM-QPSK systems," IEEE Photonics Technol. Lett. **22**, 1129–1131 (2010).
5. S. Kilmurray, T. Fehenberger, P. Bayvel, and R. I. Killey, "Comparison of the nonlinear transmission performance of quasi-Nyquist WDM and reduced guard interval OFDM," Opt. Express **20**, 4198–4205 (2012).
6. H. N. Tan, T. Inoue, T. Kurosu, and S. Namiki, "Transmission and pass-drop operations of mixed baudrate Nyquist OTDM-WDM signals for all-optical elastic network," Opt. Express **21**, 20313–20321 (2013).
7. H. N. Tan, T. Inoue, K. Tanizawa, T. Kurosu, and S. Namiki, "All-optical nyquist filtering for elastic OTDM signals and their spectral defragmentation for inter-datacenter networks," in *European Conference on Optical Communication (ECOC),* (IEEE, 2014), pp. 1–3.
8. H. Trees, *Detection, Estimation and Modulation Theory, Part 1* (Wiley, 1968).
9. P. S. Henry, "Error-rate performance of optical amplifiers," in *Optical Fiber Communications Conference and Exhibition (OFC),* (Optical Society of America, 1989), p. THK3.
10. D. Caplan and W. Atia, "A quantum-limited optically-matched communication link," in *Optical Fiber Communications Conference and Exhibition (OFC),* (IEEE, 2001), p. MM2.
11. P. J. Winzer, M. Pfennigbauer, M. M. Strasser, and W. R. Leeb, "Optimum filter bandwidths for optically preamplified NRZ receivers," J. Light. Technol. **19**, 1263–1273 (2001).
12. M. Strasser, M. Pfennigbauer, M. Pauer, and P. J. Winzer, "Experimental verification of optimum filter bandwidths in direct-detection (N) RZ receivers limited by optical noise," in *14th Annual Meeting of Lasers and Electro-Optics Society (LEOS),* (IEEE, 2001), pp. 485–486.
13. P. J. Winzer and A. Kalmár, "Sensitivity enhancement of optical receivers by impulsive coding," J. Light. Technol. **17**, 171–177 (1999).
14. M. M. Strasser, P. J. Winzer, and A. Napoli, "Noise and intersymbol-interference properties of OTDM and ETDM receivers," IEEE Photonics Technol. Lett. **16**, 248–250 (2004).
15. S. Randel, J. K. Fischer, A. M. de Melo, and K. Petermann, "Equivalent low-pass model for OTDM receivers," IEEE Photonics Technol. Lett. **17**, 1070–1072 (2005).

Optics EXPRESS

16. Z. Geng, B. Corcoran, A. Boes, A. Mitchell, L. Zhuang, Y. Xie, and A. J. Lowery, "Mitigation of electrical bandwidth limitations using optical pre-sampling," in *Optical Fiber Communications Conference and Exhibition (OFC),* (IEEE, 2017), pp. 1–3.
17. A. J. Lowery, J. Schröder, and L. B. Du, "Flexible all-optical frequency allocation of OFDM subcarriers," Opt. Express **22**, 1045–1057 (2014).
18. B. Corcoran, Z. Geng, V. Rozental, and A. J. Lowery, "Cyclic spectra for wavelength-routed optical networks," Opt. Lett. **42**, 1101–1104 (2017).
19. B. Corcoran, C. Zhu, B. Song, and A. J. Lowery, "Folded orthogonal frequency division multiplexing," Opt. Express **24**, 29670–29681 (2016).
20. H. Hu, D. Kong, E. Palushani, J. D. Andersen, A. Rasmussen, B. M. Sørensen, M. Galili, H. C. H. Mulvad, K. J. Larsen, and S. Forchhammer, "1.28 Tbaud Nyquist signal transmission using time-domain optical Fourier transformation based receiver," in *CLEO: Science and Innovations,* (Optical Society of America, 2013), pp. CTh5D–5.
21. L. Zhuang, C. Zhu, B. Corcoran, M. Burla, C. G. H. Roeloffzen, A. Leinse, J. Schröder, and A. J. Lowery, "Sub-GHz-resolution C-band Nyquist-filtering interleaver on a high-index-contrast photonic integrated circuit," Opt. Express **24**, 5715–5727 (2016).
22. Z. Geng, L. Zhuang, B. Corcoran, B. Foo, and A. J. Lowery, "Full C-band Nyquist-WDM interleaver chip," in *Optical Fiber Communications Conference and Exhibition (OFC),* (IEEE, 2017), pp. 1–3.
23. B. Corcoran, Z. Geng, V. Rozental, L. Zhuang, M. Lillieholm, and A. Lowery, "Photonic-chip-enabled 25 Tb/s optical superchannel using cyclic spectra," in *European Conference on Optical Communication (ECOC),* (IEEE, 2017), p. M.1.F.3.
24. M. A. Soto, M. Alem, M. A. Shoaie, A. Vedadi, C.-S. Brès, L. Thévenaz, and T. Schneider, "Optical sinc-shaped Nyquist pulses of exceptional quality," Nat. Commun. **4**, 3898 (2013).
25. J. Zhang, J. Yu, Y. Fang, and N. Chi, "High speed all optical Nyquist signal generation and full-band coherent detection," Sci. Rep. **4**, 6156 (2014).
26. A. J. Lowery, Y. Xie, and C. Zhu, "Systems performance comparison of three all-optical generation schemes for quasi-Nyquist WDM," Opt. Express **23**, 21706–21718 (2015).
27. M. M. Strasser, P. J. Winzer, and A. Napoli, "Noise and intersymbol-interference properties of OTDM and ETDM receivers," IEEE Photonics Technol. Lett. **16**, 248–250 (2004).
28. L. Zhuang, C. Zhu, Y. Xie, M. Burla, C. G. Roeloffzen, M. Hoekman, B. Corcoran, and A. J. Lowery, "Nyquist-filtering (de) multiplexer using a ring resonator assisted interferometer circuit," J. Light. Technol. **34**, 1732–1738 (2016).
29. P. Marin-Palomo, J. N. Kemal, M. Karpov, A. Kordts, J. Pfeifle, M. H. Pfeiffer, P. Trocha, S. Wolf, V. Brasch, and M. H. Anderson, "Microresonator-based solitons for massively parallel coherent optical communications," Nature **546**, 274 (2017).
30. R. Salem, M. A. Foster, A. C. Turner-Foster, D. F. Geraghty, M. Lipson, and A. L. Gaeta, "High-speed optical sampling using a silicon-chip temporal magnifier," Opt. Express **17**, 4324–4329 (2009).
31. L. Zhuang, C. Zhu, B. Corcoran, Z. Geng, B. Song, and A. Lowery, "On-chip optical sampling using an integrated SOA-based nonlinear optical loop mirror," in *European Conference on Optical Communication (ECOC),* (VDE, 2016), pp. 1–3.
32. M. Westlund, H. Sunnerud, M. Karlsson, and P. A. Andrekson, "Software-synchronized all-optical sampling for fiber communication systems," J. Light. Technol. **23**, 1088 (2005).
33. J. K. Fischer, R. Ludwig, L. Molle, C. Schmidt-Langhorst, C. C. Leonhardt, A. Matiss, and C. Schubert, "High-speed digital coherent receiver based on parallel optical sampling," J. Light. Technol. **29**, 378–385 (2011).
34. X. Chen, I. Kim, G. Li, H. Zhang, and B. Zhou, "Coherent detection using optical time-domain sampling," in *Optical Fiber Communications Conference and Exhibition (OFC),* (Optical Society of America, 2008), p. JThA62.